X-ray resonant scattering involving dissociative states

Faris Gelmukhanov* and Hans Ågren
Institute of Physics and Measurement Technology, Linköping University, S-58183 Linköping, Sweden
(Received 27 December 1995)

Time-independent and time-dependent theory of radiative and nonradiative resonant x-ray scattering (RXS) involving dissociative molecular states is presented. A strong space correlation between excitation and decay is found. This space correlation has a characteristic length equal to the path propagated during the lifetime of the core-excited state. It is shown that for internuclear distances beyond this characteristic length the RXS signal grows exponentially small. Additional untrivial properties of the RXS cross section for continuum-bound or bound-continuum decay transitions are predicted. Selection rules operate for continuum-bound transitions if the slope of the continuum potential is small; only transitions to vibrational states with odd quantum numbers are allowed in the harmonic approximation. We show that the main contribution to the RXS cross section is obtained at the dissociative limit if the lifetime of the core-excited state is sufficiently long. Emission transitions in the molecular region form the wing of the dissociative resonances. The spectral shape of this wing is in general oscillatory. The cross sections for both type of transitions are proportional to the square of the wave function of the vibrational state involved in the RXS process. The spectral shape copies the space distribution of the square of this wave function, and so, indirectly, maps the shape of the corresponding molecular potential. The zeros of the RXS cross section caused by the nodes of the vibrational wave function can be used to assign vibrational states. The spectral width of the RXS resonances involving dissociative molecular states strongly depends on the features of the interatomic potentials. In the general case the spectral shapes consist of a narrow part and a broad background, and will be determined by different limiting factors, such as the spectral photon shape, the Franck-Condon vibrational distribution, and the lifetime width for the core-excited states. The role of these limiting factors depends on the different combinations of dissociative and bound potentials for the ground state, the core-excited state, and the optically excited state. [S1050-2947(96)03707-9]

PACS number(s): 33.20.Rm, 33.50.Dq, 33.70.Jg, 34.50.Gb

I. INTRODUCTION

The quality of resonant core electron spectroscopies in the x-ray region has advanced to a point where the fine structure and spectral shapes can fingerprint the dynamical history of the full scattering process. The coupling between electronic and nuclear motions and the time scales describing excitation, decay, and, eventually, dissociation in the connected potentials have now become relevant concepts for the interpretation of high-resolved x-ray scattering spectra. In addition to a trivial general broadening by the spectrometer, the measured x-ray line shape will result from an interplay between the shapes of several functions: the photon function, the lifetime broadening function, and the vibrational (discrete or continuous) distribution function. This interplay will in turn be dependent on the character of the participating states, if they are bound or dissociative. With the development of tunable, narrow-band synchrotron-radiation sources [1–6], studies of the resonant x-ray scattering process are no longer limited to systems with discrete bound states but now also involve systems with states that are unbound along the nuclear degrees of freedom.

The diatomic hydrides served as the original prototypes for resonance Auger (nonradiative x-ray) spectra involving dissociative states. Decay channels with dissociation preceding electronic decay were first identified in the spectrum of HBr recorded at the $3d\to\sigma^*$ excitation energy [7]. The HCl $2p\to\sigma^*$ resonance was also found to decay predominantly by dissociation followed by the electronic decay [8]. The time scales of the dissociation and the Auger decay were estimated to be of the same order of magnitude [7], but even the simultaneous coexistence of molecular and atomic Auger spectra has been predicted [8]. The H_2S molecule served, to our knowledge, as the first polyatomic species showing similar features [9,10]. Studies of this species clearly indicated that the character of the core-excited state determines the relaxation path, and that dissociation before decay is possible even for short-lived core hole states. The $2p$ absorption spectra in this molecule, as in HCl, exhibit a preedge structure [11,9] consisting of a broad band due to excitations to the first unoccupied molecular orbital ($6a_1$ and $3b_2$ in the case of H_2S, 6σ or ''σ^*'' for HCl) followed by a series of sharp peaks corresponding to excitations to Rydberg orbitals. The identification of the Auger spectra for the various excitation energies indicated that the first type of excited states relaxed through Auger transitions in dissociative fragments, while excitations to the bound Rydberg states showed resonance Auger decay in the molecular environment. Calculations on core-excited adiabatic interatomic potentials of different molecules, for example O_2 [12,13], HBr [14], HCl [8], and H_2S [9], confirm that intermediate or final states with dissociative character are indeed relevant to consider for the RXS process.

Experimental conclusions about the relaxation paths of the core-excited states thus followed from energy assignments of the Auger decay spectra. These spectra were inter-

*Permanent address: Institute of Automation and Electrometry, 630090 Novosibirsk, Russia.

pretable in terms of diagram levels of the fragments. The assignments, the excitation energy dependencies, and mass spectroscopic data gave hints of a mechanism in which dissociation is faster than the electronic decay of the excited fragment. From further experimental progress with synchrotron radiation, it has also been possible to use line shapes and the Auger resonance Raman effect [15–17] to draw conclusions on the character of the intermediate and also the final states [18–20]. Only the bound states showed the expected resonance narrowing of the bands (Raman effect), while the Auger transitions to final dissociative states lacked such narrowing and were determined by their lifetime broadening only.

Although classical or semiclassical estimates of the time scales for the relaxation have been useful, basic theories for x-ray resonant scattering involving dissociative states have not been provided in a way that matches the theory for bound discrete states. Theory now covers a cross section of interesting effects for RXS involving discrete states in atoms [16], molecules [21–23], and solids [24,4,25]. Radiative and nonradiative RXS involving bound discrete vibrational levels have been investigated to a rather large extent, experimentally [26–28] and theoretically [29,30,26,31,32]. These investigations have uncovered the strong influence of interference between intermediate vibrational levels on the spectral shape of the RXS signals. Many, if not most, molecular core-excited states are dissociative or predissociative, and it is desirable to include these in a general treatment. The interference effect will also be a central concept in such a treatment.

With the present paper we intend to investigate the conditions for resonant x-ray (Raman) spectroscopy involving dissociative states, and derive general expressions for the observed non-spectrometer-broadened spectral function. The starting point and main emphasis rest on time-independent theory, with a time-dependent approach used as an interpretative complement for the kinematic and dynamic aspects, and to explore when ''dissociation before decay'' is possible. The paper is organized as follows. The time-independent theory of resonant x-ray scattering involving dissociative states is presented in Sec. II. In Sec. II A the space correlation between the absorption and emission processes is investigated. Section II B presents a general analysis of continuum-continuum and bound-continuum Franck-Condon factors. The energy dependence of the RXS cross sections are given in Sec. II C. As is shown here, there exists a deep connection between the interference of the continuum states and the damping of emission for large internuclear distances. The spectral features of x-ray fluorescence and resonant Auger spectra involving dissociative states are discussed in Sec. II D, separating the cases of different combinations of bound and continuum potentials. The limiting factors for the spectral shape are derived for each such case. The interplay between the narrow resonance and the broad background parts and the oscillatory behavior of the background are also discussed in that connection. A direct mapping of the (square) of the vibrational wave functions of a bound intermediate state is another important result discussed in this section. A complementary time-dependent treatment of RXS is given in Sec. III. Here the ''E coherence'' and ''t coherence,'' and the ''E interference'' and ''t interference'' concepts are introduced, and their special relations for different experimental situations are derived. The last section, Sec. IV, summarizes our findings.

II. RESONANT X-RAY SCATTERING INVOLVING DISSOCIATIVE STATES. TIME-INDEPENDENT THEORY

Resonant x-ray scattering is commonly described as a one-step process involving three states: the initial, intermediate, and final states. The latter can be identical with—or excited with respect to—the initial state, describing elastic and inelastic scattering, respectively. Being in the x-ray region the intermediate state is in general core excited and therefore short lived; our theory nevertheless also covers the long-lived limit. In principle one can consider any combination of bound and dissociative characters of these states; however, we confine ourselves to the experimental situation with stable ground-state molecules only, allowing for dissociative character of the intermediate or final states, or of both these states. We impose the important restriction of having only one nuclear degree of freedom, i.e., a diatomic molecule characterized by the interatomic distance R.

To outline a time-independent formulation of the RXS cross sections, we start from the generalized Kramers-Heisenberg formulas for inelastic (RIXS) and elastic (REXS) x-ray scattering cross section

$$\sigma^{\mathrm{tot}}(\omega',\omega)=\sigma^{\mathrm{RIXS}}(\omega',\omega)+\sigma^{\mathrm{REXS}}(\omega',\omega). \tag{1}$$

Unless otherwise stated use atomic units ($\hbar=m=e=1$, $\alpha=1/137$). The first term on the right-hand side of this equation,

$$\sigma^{\mathrm{RIXS}}(\omega',\omega)=\frac{\omega'}{\omega}\sum_f |F_f|^2\Delta(\omega-\omega'-\omega_{f_0},\gamma_0),$$
$$F_f=\sum_c \frac{\langle f|Q|c\rangle\langle c|V|0\rangle}{\omega-\omega_{c0}+i\Gamma},\quad \Delta(\omega,\Gamma)=\frac{\Gamma}{\pi(\omega^2+\Gamma^2)}, \tag{2}$$

describes the inelastic scattering, while the second term,

$$\sigma^{\mathrm{REXS}}(\omega',\omega)=|F_0|^2\delta(\omega'-\omega),$$
$$F_0=\sum_c \frac{\langle 0|V'|c\rangle\langle c|V|0\rangle}{\omega-\omega_{c0}+i\Gamma}, \tag{3}$$

appearing only in radiative RXS, is responsible for elastic scattering. Here ω and ω' are the frequencies of incoming and outgoing x-ray photons, respectively, γ_0 is the lifetime of the final state, V and V' are the operators for the dipole interaction of incoming and outgoing x-ray photons with the molecule, Q is the Coulomb-interaction-operator-induced Auger decay in nonradiative RXS, and $Q=V'$ for radiative RXS. E_c, $|c\rangle$ and E_f, $|f\rangle$ are eigenvalues and eigenfunctions of the core-excited and final-state Hamiltonians H_c and H_f, and $\omega_{f0}=E_f-E_0$. It is necessary to note that in strict theory the Hamiltonians H_c and H_f are identical and equal to the total molecular Hamiltonian. For brevity we refer below to RXS as radiative x-ray scattering, and let ω' denote the final photon frequency. The only change for a nonradiative RXS

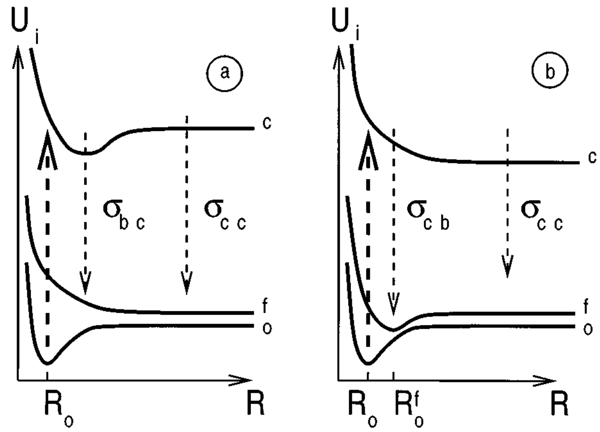

FIG. 1. Excitation and decay schemes. The ground (0), intermediate (c), and final (f) states are displaced relative to each other. All notations are explained in the text.

description is that the frequency of the final photon ω' must be replaced by the energy of the Auger electron.

The frequency ω' of the x-ray emission photons has a Raman-related shift (Stokes shift) toward the long-wavelength region relative to the frequency ω of the absorbed photon $\omega=\omega'+\omega_{f0}$, in accordance with the energy conservation law and the Lorentzian function in Eq. (2). This Raman-related shift leads to the earlier predicted Stokes doubling effect in radiative [21] and nonradiative RIXS [33,34] processes, which was recently observed in resonant Auger spectra of krypton [20]. When interpreting experiments, we use the convolution

$$\overline{\sigma(\omega',\omega_c)}=\int \sigma(\omega',\omega)\Phi(\omega-\omega_c,\gamma)d\omega \qquad (4)$$

of the RXS cross section with the incoming photon distribution function $\Phi(\omega-\omega_c,\gamma)$ centered at frequency ω_c and having a width γ.

Let us begin the investigation of this problem for the special case when the incoming x-ray photon excites the molecule to an intermediate dissociative state (Fig. 1). We assume excitation to the adiabatic interatomic potential $U_c(R)$ of a dissociative state [or above dissociation threshold if $U_c(R)$ is at a minimum]. As is shown in Fig. 1 two qualitatively different channels for the radiative decay exist. One is the decay from an intermediate continuum nuclear state $|c\rangle=\varphi^c_{E_c}(R)$ to a bound vibrational state $|f\rangle=\varphi^f_m(R)$ of the final internuclear potential $U_f(R)$. Here E_c is the molecular energy of the continuum state $\varphi^c_{E_c}(R)$. This channel will be called the continuum-bound channel. The second channel is given by the decay into final dissociative states $|f\rangle=\varphi^f_{E_f}(R)$, the continuum-continuum channel. We can rewrite cross section (2) for the considered case as the sum of cross sections $\sigma_{\rm cb}(\omega',\omega)$ and $\sigma_{\rm cc}(\omega',\omega)$ for the continuum-bound and continuum-continuum decay channels:

$$\sigma(\omega',\omega)=\sigma_{\rm cb}(\omega',\omega)+\sigma_{\rm cc}(\omega',\omega),$$

$$\sigma_{\rm cb}(\omega',\omega)=\frac{\omega'}{\omega}\sum_m |F_{f(m)}|^2\delta(\omega'-\omega+\omega_{m0}), \qquad (5)$$

$$\sigma_{\rm cc}(\omega',\omega)=\frac{\omega'}{\omega}|F_f|^2.$$

Here the Dirac δ function is used instead of the Lorentzian function due to the smallness of the final-state lifetime broadening γ_0. The energy conservation law yields the following expression for the molecular energy E_f of the continuum state $\varphi^f_{E_f}(R)$:

$$E_f=\omega-\omega'+E_0. \qquad (6)$$

The RXS cross section (5) makes two qualitatively different contributions: one of them, $\sigma_{\rm cb}$, is sharp, while the other, $\sigma_{\rm cc}$, has a smooth frequency dependence. It is necessary to remember that both contributions to σ have additional broadenings caused by the finite width of the incoming photon spectral distribution on top of the instrumental broadening (4). The spectral width of the incoherent part of the cross section $\sigma_{\rm cc}$ is defined by the width of the continuum scattering amplitude F_f. The spectral distribution of F_f is given by the spectral distribution of the Franck-Condon factors, as further studied in Sec. II A.

In the common Born-Oppenheimer and Condon approximations the transition matrix elements Q and V are treated as constants instead of as functions of the nuclear coordinates, and the scattering amplitudes for the continuum-continuum F_f and for continuum-bound $F_{f(m)}$ channels simplify to [29–31].

$$F_{f,f(m)}=VQ\sum\int dE_c\,\frac{\langle\varphi^f_{E_f,m}|\varphi^c_{E_c}\rangle\langle\varphi^c_{E_c}|\varphi_0\rangle}{\omega-\omega_{c0}+i\Gamma}, \qquad (7)$$

where $\omega_{c0}=E_c-E_0$. The continuum nuclear wave functions of states $i=c,f$ are here normalized to a δ-energy function:

$$\langle\varphi^i_{E_i}|\varphi^i_{E'_i}\rangle=\delta(E_i-E'_i). \qquad (8)$$

The sum on the right-hand side of Eq. (7) implies that for a bound intermediate state $|c\rangle$ one needs to integrate over the energy E_c or sum over the vibrational states φ^c_n if the incoming photon frequency is tuned above or below the dissociation threshold of the intermediate state, respectively. The scattering amplitude (7) is defined by Franck-Condon (FC) factors (the overlap integrals) between the vibronic wave function $\varphi_0(R)$ of the ground state and the continuum nuclear wave functions $\varphi^c_{E_c}(R)$, and between $\varphi^c_{E_c}(R)$ and the final-state nuclear wave functions $\varphi^f_{E_f}(R)$.

A. Space correlation between absorption and emission

At this stage we focus on the fundamental role that interference between different intermediate continuum states

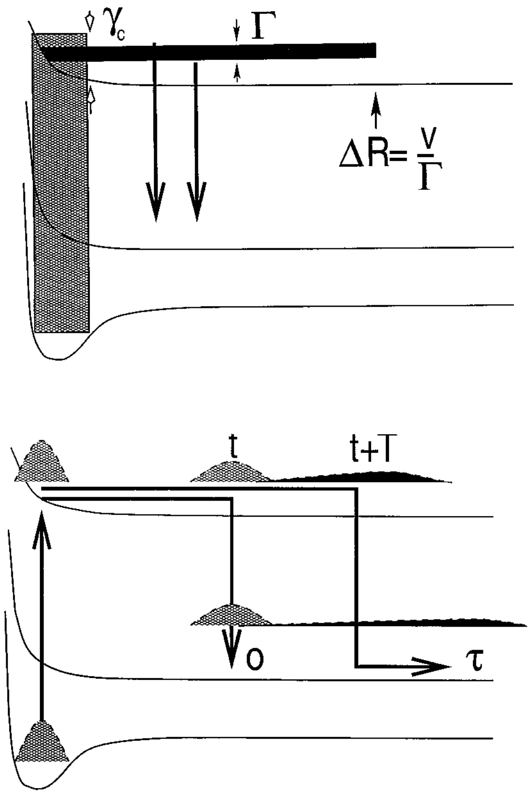

FIG. 2. Illustration of E interference (upper panel) and t interference (lower panel). $\Delta R = R' - R$ is the distance between absorption (R) and emission (R') points. v is the characteristic nuclear velocity. All notations are explained in the text.

plays in the damping of emission as the internuclear distance increases. To give a general treatment of this problem, let us rewrite the scattering amplitude (7)

$$F_f = \langle \varphi^f_{E_f} | \tilde{\varphi}_c \rangle$$
$$= VQ \int_{-\infty}^{\infty} \int_{-\infty}^{\infty} dR' dR \; \varphi^{f*}_{E_f}(R') G^+_E(R',R) \varphi_0(R) \quad (9)$$

in terms of the stationary wave packet $\tilde{\varphi}_c(R)$ and the time-independent Green's function

$$\tilde{\varphi}_c = G^+_E \varphi_0, \quad G^+_E(R',R) = \int dE_c \, \frac{\varphi^{c*}_{E_c}(R') \varphi^c_{E_c}(R)}{E - E_c + i\Gamma}, \quad (10)$$

with $E = \omega + E_0$. The stationary lifetime-broadened Green's function $G^+_E(R',R)$ describes the propagation of nuclei on a decaying potential surface $U_c(R)$ from the internuclear distance R, where the molecule was core excited up to R' where the emission transition took place. When the core-excited state is short lived, $\Gamma \gg U(R_0) - U_c(R_{cf})$ (26), the Green's function

$$G^+_E(R',R) = \frac{\delta(R'-R)}{E - U_c(R_0) + i\Gamma} \quad (11)$$

shows that the emission and absorption transitions take place at the same point ($\Delta R = R' - R = 0$) (Fig. 2, upper panel). Thus in the limit of zero lifetime the molecule has no time to spread from the point of absorption. The finite lifetime broadening Γ means that the core excitation cuts off the coherent superposition $\tilde{\varphi}_c$ (10) of the core-excited states residing in an energy bandwidth given by the lifetime broadening $|E_c - E| \leqslant \Gamma$ (Fig. 2). When Γ is large all intermediate states ($|E_c - E| \leqslant \infty$) make coherent contributions to the wave packet $\tilde{\varphi}_c$ (maximum interference between core-excited states). In this case the point of emission is known exactly ($R' = R$, $\Delta R \to 0$) according to Eq. (11). The x-ray excitation cuts off only a small part ($|E_c - E| \leqslant \Gamma \to 0$) of the continuum intermediate states if Γ is small (Fig. 2). Hence according to the uncertainty principle the $\delta(R'-R)$ function in Eq. (11) is broadened, and the explicit information about the emission point R' is lost ($\Delta R \to \infty$) (Fig. 2).

To obtain a deeper understanding of the case of finite Γ let us look at the lifetime-broadened Green's function (10). In the relevant region the nuclei move with an energy E_c larger than the potential height $U_c(R)$. So the criterion of applicability of the quasiclassical approximation is fulfilled everywhere, and the quasiclassical wave function can be written as

$$\varphi^c_{E_c}(R) = \frac{A}{\sqrt{p_c(R)}} \exp\left(-i \int_a^R p_c(R') dR' \right). \quad (12)$$

Here $p_c(R) = \sqrt{2\mu(E_c - U_c(R)}$ is the momentum, a is the classical turning point where $p_c(a) = 0$, and A is the normalization constant. The small correction term containing the wave reflected by inhomogeneities of the potential is neglected in Eq. (12). In the classically accessible region (R', $R \geqslant a$), and in $R' \geqslant R$ the lifetime-broadened Green's function shows strong space correlation between the absorption and emission processes,

$$G^+_E(R',R) = G^{(0)+}_E(R',R) e^{-2\Gamma\tau(R',R)},$$

$$G^{(0)+}_E(R',R) = -2i\pi A^2 \, \frac{\exp(i\int_R^{R'} p(R'')dR'')}{\sqrt{\overline{p(R')}\,\overline{p(R)}}}, \quad (13)$$

where $\overline{p(R)} = p(R) + i\Gamma/v(R)$, $p(R) = \sqrt{2\mu(E - U_c(R)}$, and $v(R) = p(R)/\mu$ is the relative velocity of the nuclei at the point R. The lifetime broadening Γ is here assumed to be small in comparison with $[E - U_c(R)]$. As follows from the factor $\exp[-2\Gamma\tau(R',R)]$ in Eq. (13), the emission intensity is negligible if the time of propagation between the absorption point (R) and the emission point (R'),

$$\tau(R',R) = \int_R^{R'} \frac{dR''}{v(R'')}, \quad (14)$$

exceeds the lifetime: $\tau(R',R) \geqslant \Gamma^{-1}$. Indeed, the emission takes place only until the population of the core-excited state remains unexhausted. So we obtain that the internuclear distance $|R' - R|$ between absorption and emission points cannot exceed the distance (v/Γ) passed by the nuclei during the lifetime (Fig. 2):

$$|R' - R| \leqslant v/\Gamma. \quad (15)$$

We can now conclude that the damping factor $\exp[-2\Gamma\tau(R',R)]$ is caused by the interference between the core-excited continuum states $\varphi^c_{E_c}(R)$ coherently excited into the band $|E_c-E|\leqslant\Gamma$. So this interference between continuum states and the finite value of Γ plays the key role in the damping of x-ray emission at large internuclear distances.

B. Analysis of Franck-Condon factors

Let us estimate the first Franck-Condon factor $\langle\varphi^c_{E_c}|\varphi_0\rangle$ in Eq. (7) between continuum vibrational wave functions of the intermediate core-excited electronic state and the ground-state vibrational wave function, for example, in the harmonic approximation

$$\varphi_0(x)=\left(\frac{1}{\pi a_0^2}\right)^{1/4}\exp\left[-\frac{1}{2}\left(\frac{x}{a_0}\right)^2\right],\quad a_0=\left(\frac{\hbar}{\mu\omega_0}\right)^{1/2}, \tag{16}$$

where μ is the reduced mass, ω_0 the vibrational frequency, and a_0 has the meaning of an average deviation of $x=R-R_0$ from the equilibrium R_0 of the ground state. In accordance with the Franck-Condon principle the main contribution to $\langle\varphi^c_{E_c}|\varphi_0\rangle$ is given by the region close to the ground-state equilibrium R_0, where $\varphi_0(x)$ is localized. We now expand the interatomic potential $U_c(R)$ near R_0 over the displacement $x=R-R_0$: $U_c(R)=U_c(R_0)-\mathcal{F}_{c0}x$. Here $\mathcal{F}_{c0}=-(dU_c/dR)_0$ is the interatomic force at the equilibrium point R_0. The finite regular solution of the Schrödinger equation with a linear potential is given by the Airy function [35,36]

$$\varphi^c_{E_c}=\sqrt{2\mu a_{c0}}\mathrm{Ai}(-\zeta),\quad \mathrm{Ai}(x)=\frac{1}{\pi}\int_0^\infty ds\ \cos[\tfrac{1}{3}s^3+xs], \tag{17}$$

where

$$\zeta=\frac{1}{a_{c0}}(x-x_{c0}),\quad x_{c0}=-\frac{\epsilon_{c0}}{\mathcal{F}_{c0}},$$
$$a_{c0}=\left(\frac{\hbar^2}{2\mu\mathcal{F}_{c0}}\right)^{1/3},\quad \epsilon_{c0}=E_c-U_c(R_0). \tag{18}$$

x_{c0} is the classical turning point for the linear potential $U_c(R)=U_c(R_0)-\mathcal{F}_{c0}x$. The characteristic scale of oscillations a_{c0} of the Airy function decreases if the potential slope $\mathcal{F}_{c0}$ at the equilibrium point R_0 increases. When the slope $\mathcal{F}_{c0}$ is large ($a_{c0}/a_c<1$) the Airy function $\mathrm{Ai}(-\zeta)$ oscillates strongly if $\zeta>0$ and decreases quickly if $\zeta<0$. This leads to the following estimation for the FC factor:

$$\langle\varphi^c_{E_c}|\varphi_0\rangle\simeq\sqrt{2\mu a_{c0}^3}\varphi_0\left(\frac{-\Delta\epsilon_c}{\mathcal{F}_{c0}}\right)\simeq\left(\frac{2\mu a_{c0}^3}{\pi^{1/2}a_0}\right)^{1/2}\times\exp\left[-\frac{1}{2}\left(\frac{\Delta\epsilon_c}{\gamma_c}\right)^2\right],$$
$$\Delta\epsilon_c=\epsilon_{c0}+\mathcal{F}_{c0}a_{c0},\quad \gamma_c=\mathcal{F}_{c0}a_0, \tag{19}$$

where the right-hand side expression is obtained from the harmonic approximation. This bound-continuum FC factor describes the energy distribution of the intermediate continuum nuclear states. The width γ_c of this distribution is the product of the width a_0 of $\varphi_0(x)$ and the slope $\mathcal{F}_{c0}$ [37]. The expression for γ_c also follows from geometrical considerations [37,38]. The same estimation is valid for the continuum-bound FC factor ($\varphi^c_{E_c}\to\varphi^f_m$ transition)

$$\langle\varphi^f_m|\varphi^c_{E_c}\rangle\simeq\sqrt{2\mu\tilde{a}_{c0}^3}\varphi^f_m\left(-\frac{\Delta\tilde{\epsilon}_c}{\tilde{\mathcal{F}}_{c0}}\right)\simeq\left(\frac{2\mu\tilde{a}_{c0}^3}{\pi^{1/2}\tilde{a}_02^m m!}\right)^{1/2}\times\exp\left[-\frac{1}{2}\left(\frac{\Delta\tilde{\epsilon}_c}{\tilde{\gamma}_c}\right)^2\right]H_m\left(-\frac{\Delta\tilde{\epsilon}_c}{\tilde{\gamma}_c}\right), \tag{20}$$

where $H_m(x)$ is the Hermite polynomial. The final-state potential $U_f(R)$ is approximated here by a harmonic potential with minimum in R_0^f. For brevity, in Eq. (20) we kept the notations of Eq. (19), marking our parameters by the tilde symbol. Contrary to the previous parameters given by Eqs. (16), (18), and (19), the tilde-marked parameters are obtained at the equilibrium point R_0^f of the final-state potential $U_f(R)$. $\tilde{\omega}_0$ is the vibrational frequency of the final-state potential $U_f(R)$.

When $\tilde{a}_0/\tilde{a}_{c0}\ll1$ the vibrational wave function φ^f_m of the bound state is narrower than the Airy function, implying the following approximation for the continuum-bound FC factor:

$$\langle\varphi^f_m|\varphi^c_{E_c}\rangle\simeq\sqrt{2\mu\tilde{a}_{c0}}\mathrm{Ai}\left(-\frac{\Delta\tilde{\epsilon}_c}{\tilde{\mathcal{F}}_{c0}\tilde{a}_{c0}}\right)\int_{-\infty}^{\infty}\varphi^f_m(x)dx. \tag{21}$$

The integral on the right-hand side of this equation shows that in the case of a harmonic potential the bound-continuum and continuum-bound transitions are forbidden for odd m. It is important to note that the expression for the continuum-bound FC factors (19) and (20) between the bound vibrational wave functions $\varphi_0(R)$ and $\varphi^f_m(R)$ is valid for arbitrary bound wave functions (thus not only for the Hermite polynomials). Equations (19) and (20) can also be obtained in the reflection approximation [39], where the continuum wave function is replaced by $\delta(x-x_0)$, with x_0 as the classical turning point.

Let us now consider the spectral region with decay transitions into final continuum states $\varphi^f_{E_c}$ lying above the dissociation threshold of the final state potential $U_f(\infty)$ (continuum-continuum decay channel). To estimate the scattering amplitude in this case we assume that the internuclear distance remains unaltered during the electron transition $c\to f$ (vertical approximation). Suppose that this transition takes place at points R near some internuclear distance R_{cf}. Only such points can make significant contributions to the FC factors. The solutions of the Schrödinger equations for the intermediate and final nuclear states near this stationary point R_{cf} are given by Airy functions (17) with parameters corresponding to this point.

Let us now direct attention to the continuum wave function of the core-excited state. We will use different Airy forms (17) of $\varphi^c_{E_c}$ to evaluate absorption $\langle\varphi^c_{E_c}|0\rangle$ and emission $\langle\varphi^f_{E_f}|\varphi^c_{E_c}\rangle$ FC factors. Since these Airy solutions near R_0 and R_{cf} approximate the same wave function $\varphi^c_{E_c}$, they are connected with each other by the phase multiplier $\exp(i\vartheta)$ with the phase shift estimated as

$$\vartheta \simeq \int_{a(R_0)}^{R_{cf}} p_c(R)dR. \tag{22}$$

Here $a(R_0)$ is the classical turning point lying near R_0. The nuclear momentum $p_c(R)=\sqrt{2\mu[E_c-U_c(R)]}$ is equal to zero at this point. Estimation (22) follows from the connection between the quasiclassical continuum wave function in different points and the condition $a_0, a_{c0} \ll R_0, R_{cf}$.

Taking into account the properties of the Airy function [35,36] and the phase factor $\exp(i\vartheta)$, one arrives at the following expression for the continuum-continuum overlap integral:

$$\langle \varphi^f_{E_f}|\varphi^c_{E_c}\rangle = e^{i\vartheta}\begin{cases} \delta(\epsilon_f-\epsilon_c) & \text{if} \quad \mathcal{F}_f=\mathcal{F}_c \\ \dfrac{1}{\gamma_{cf}}\,\mathrm{Ai}\left\{\pm\dfrac{1}{a}\left(\dfrac{\epsilon_f}{\mathcal{F}_f}-\dfrac{\epsilon_c}{\mathcal{F}_c}\right)\right\} & \text{if} \quad \mathcal{F}_f\neq\mathcal{F}_c, \end{cases} \tag{23}$$

with

$$\gamma_{cf}=a\mathcal{F}=\left|\frac{\hbar^2}{2\mu}(\mathcal{F}_f-\mathcal{F}_c)\mathcal{F}\right|^{1/3}, \quad a=\sqrt{a_f a_c}\left|\frac{\mathcal{F}_f-\mathcal{F}_c}{\mathcal{F}}\right|^{1/3},$$
$$\mathcal{F}=\sqrt{\mathcal{F}_c\mathcal{F}_f}, \quad a_i=\left(\frac{\hbar^2}{2\mu\mathcal{F}_i}\right)^{1/3}. \tag{24}$$

The slope $\mathcal{F}_i=-(dU_i/dR)$ and the kinetic nuclear energy $\epsilon_i=E_i-U_i(R)$ of states $i=c,f$ are calculated at the stationary point $R=R_{cf}$. Equation (23) is written for $\mathcal{F}_i>0$. The $+$ and $-$ signs in the argument of the Airy function (23) should be used for the cases $\mathcal{F}_f>\mathcal{F}_c$ and $\mathcal{F}_f<\mathcal{F}_c$, respectively. The phase shift ϑ between absorption (19) and emission (23) matrix elements originates in the difference between phases of the wave function $\varphi^c_{E_c}$ at the FC points R_0 and R_{cf} of absorption and emission transitions. Phase ϑ demonstrates strong space correlation or coherence between absorption and emission, and, as will be shown below, the phase factor $\exp(i\vartheta)$ leads to important physical consequences.

In the quasiclassical limit where $\gamma_{cf}\propto\hbar^{2/3}\to 0$ (γ_{cf} being the characteristic width of the FC factors) the FC factor (23) tends to $\delta(\epsilon_f/\mathcal{F}_f-\epsilon_c/\mathcal{F}_c)$. This FC factor is maximal near the point

$$\frac{\epsilon_c}{\mathcal{F}_c}=\frac{\epsilon_f}{\mathcal{F}_f}. \tag{25}$$

In the general case the term $\pm a$ must be added to the right-hand side of this equation, because the Airy function $\mathrm{Ai}(-\zeta)$ has a maximum value $[\mathrm{Ai}(-1)\simeq 0.53]$ when $\zeta=1$.

C. Evaluation of the RXS cross sections

Let us begin from a time-independent treatment of the short-lifetime limit

$$\Gamma \gg \gamma_c,\ \gamma_{cf},\ \Delta V, \tag{26}$$

where $\Delta V=U_c(R_0)-U_c(R_\infty)$. In reality this condition ($\Gamma\gg\Delta V$) is too strong, and, as will be shown below, it is softened in the different special cases. The FC factors (19) and (23) in the numerator of the right-hand side of Eq. (7) restrict the region of allowed values of E_c to $\Delta E_c \leqslant \gamma_c, \gamma_{cf}$. So when the core-excited state is short lived (26), one can neglect the energy dependence of the denominator in the expression (7) for the RXS amplitude and extract this denominator from the integral over E_c at the point $E_c=U_c(R_0)$ according to the FC rule. Taking into account the condition of completeness, $\Sigma_c|c\rangle\langle c|=1$, one arrives at the following expression for the scattering amplitude (7):

$$F_f=\frac{VQ}{\omega-\omega_{c0}(R_0)+i\Gamma}\langle\varphi^f_{E_f}|\varphi_0\rangle, \quad \omega_{i0}(R)=U_i(R)-E_0. \tag{27}$$

If we complete Eq. (26) by the condition $\Gamma\gg\omega_0$ it is easy to see that this result [31] is general and not restricted to continuum intermediate and final states. Here ω_0 is the vibrational frequency of the bound core-excited state. A more physical point of view for this problem was given in Sec. I A [see Eq. (11)]. Equation (27), which is also obtained below in the time-dependent treatment of RXS, shows that only direct transitions between the vibrational states of ground and final states take place in the limiting case of a short lifetime. According to this equation the main contribution to the FC factor $\langle\varphi^f_{E_f}|\varphi_0\rangle$ is given at internuclear distances near the equilibrium R_0 of the ground state. In other words, the atoms in the molecule have no time to spread far from R_0 when the core-excited state is short lived. In this limiting case let us write the final expression for the continuum-continuum cross section (5), using Eqs. (19) and (27), as

$$\sigma_{\mathrm{cc}}(\omega',\omega)=\sigma\Delta(\omega'-\omega_{cf}(R_0)-\mathcal{F}_{f0}a_{f0},\Gamma)\times\exp\left[-\left(\frac{\omega-\omega'-\omega_{f0}(R_0)+\mathcal{F}_{f0}a_{f0}}{\gamma_c}\right)^2\right],$$
$$\sigma=\frac{2\pi^{1/2}\mu a_{f0}^3}{\Gamma a_0}\frac{\omega'}{\omega}|VQ|^2, \quad \omega_{cf}(R)=U_c(R)-U_f(R). \tag{28}$$

Consider now the other important limiting case, when the spectral width of the continuum-continuum FC is small, and $\mathcal{F}_c\to\mathcal{F}_f$:

$$\gamma_{cf}\ll\Gamma,\ \gamma_c. \tag{29}$$

According to $\lim_{a\to 0}\mathrm{Ai}(x/a)=a\,\delta(x)$, the FC factor (23) is then equal to

$$\langle\varphi^f_{E_f}|\varphi^c_{E_c}\rangle=e^{i\vartheta}\delta(\epsilon_f-\epsilon_c). \tag{30}$$

From Eqs. (5) and (7), we thus have the following expression for the RXS cross section in the limit (29):

$$\sigma_{\mathrm{cc}}(\omega',\omega)=\sigma\frac{\mathcal{F}_{f0}}{\mathcal{F}_{c0}}\Delta[\omega'-\omega_{cf}(R_{cf}),\Gamma]\times\exp\left[-\left(\frac{\omega-\omega'-\Omega}{\gamma_c}\right)^2\right], \tag{31}$$

where

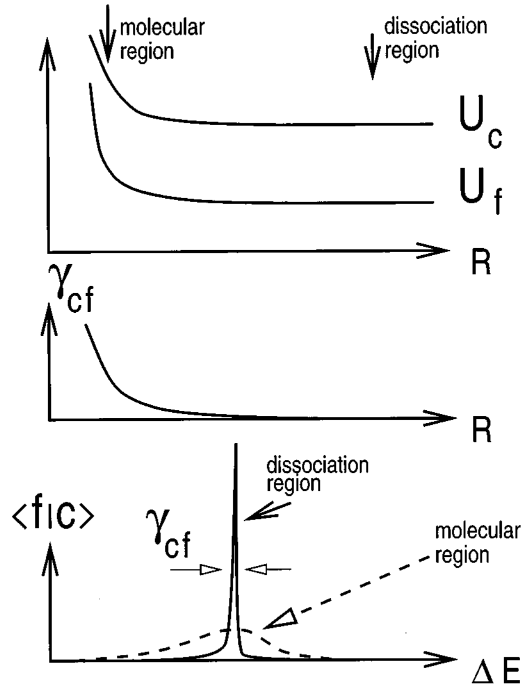

FIG. 3. Qualitative separation of the R space into molecular and dissociative regions (upper panel). The qualitative dependence of the spectral width of the continuum-continuum FC factor $\langle f|c\rangle = \langle \varphi^f_{E_f}|\varphi^c_{E_c}\rangle$ (23) on the internuclear distance R (middle panel). The qualitative dependence of the continuum-continuum FC factor (23) on the energy $\Delta E = \mathcal{F}(\epsilon_f/\mathcal{F}_f - \epsilon_c/\mathcal{F}_c)$ in the molecular and dissociative regions (lowest panel). The FC factor amplitude ($\propto 1/\gamma_{cf}$) is large in the dissociative region but small in the molecular region (the oscillatory character of the FC factor is not depicted).

$$\Omega = \omega_{c0}(R_0) - \omega_{cf}(R_{cf}) - \mathcal{F}_{c0}a_{c0}, \tag{32}$$

The same result follows directly from Eqs. (5) and (7) if the potentials $U_c(R)$ and $U_f(R)$ coincide. The continuum-continuum FC factor (23) is also equal to the δ function due to the mutual orthogonality of nuclear wave functions $\varphi^f_{E_f}$ and $\varphi^c_{E_c}$ in this case. The region of integration for the FC factor, $\langle \varphi^f_{E_f}|\varphi^c_{E_c}\rangle$, is restricted by $R' - R_0 < v/\Gamma$ according to Eq. (15) of Sec. II A. Hence Eq. (31) is true until $R_{cf} - R_0 < v/\Gamma$. The cross section $\sigma_{cc}(\omega',\omega)$ is exponentially small if the crossing point R_{cf} exceeds the passage propagated during the lifetime, v/Γ, with the characteristic velocity v (see below).

It is necessary to note the special important case when solution (31) describes the emission in the dissociative region $R_{cf}\to\infty$. Indeed, the dissociative limit resides in the region of Eq. (29) since the spectral width of the continuum-continuum FC factors (23) tends to zero ($\gamma_{cf}\to 0$) due to the slope $\mathcal{F}_i \to 0$ when $R_{cf}\to\infty$ (Fig. 3). When $\mathcal{F}_i\to 0$ the Airy solution (17) for the linear potential overestimates the role of large R where the exact potential $U_i(R)$ is negligibly small. The RXS cross section (31) for the dissociative region was therefore obtained from Eq. (23), with the additional assumption $\lim_{R\to\infty}(\mathcal{F}_c/\mathcal{F}_f)=1$.

To evaluate the RXS cross section in the intermediate region with the crossing point lying in the molecular region ($R_0 < R_{cf} < \infty$), we need to use the equation for the crossing point R_{cf} [40],

$$\omega' = \omega_{cf}(R_{cf}). \tag{33}$$

The spectral width γ_{cf} (24) of the continuum-continuum FC factor depends strongly on the difference between the slopes $\mathcal{F}_c$ and $\mathcal{F}_f$ governed by R_{cf} (Fig. 3). Two important limiting cases exist. In the first case considered above, the spectral width γ_{cf} is small in comparison with the widths of the bound-continuum FC factor (19) and the lifetime broadening. In this limit (29) the RXS cross section (31) is described by the product of a Gaussian and a Lorentzian with the spectral widths γ_c and Γ. In the opposite limiting case

$$\Gamma \ll \gamma_c,\ \gamma_{cf}, \tag{34}$$

the energy conservation law holds for the absorption transition too: $\omega=\omega_{c0}$. Because now the sharpest function in the integral (7) is $1/(\omega-\omega_{c0}+i\Gamma)$, the FC factors [except the strongly oscillating phase factor $\exp(i\vartheta)$ (22)] can be extracted from this integral at the point $E_c=\omega+E_0$. Different from the cross sections (28) and (31), the RXS cross section according to Eq. (33) now equals

$$\sigma_{cc}(\omega',\omega) = \sigma\,\frac{\pi\Gamma}{\gamma_{cf}^2}\,\frac{\mathcal{F}_{f0}\mathcal{F}_f}{\mathcal{F}_{c0}\mathcal{F}_c}\exp\left[-\left(\frac{\Delta\omega+\mathcal{F}_{c0}a_{c0}}{\gamma_c}\right)^2\right] \times \mathrm{Ai}^2\left(-\left(\frac{\Delta\omega+\delta}{\tilde{\gamma}_{cf}}\right)\right)e^{-2\Gamma\tau}, \tag{35}$$

where

$$\Delta\omega = \omega - \omega_{c0}(R_0), \quad \delta = U_c(R_0) - U_c(R_{cf}),$$
$$\tilde{\gamma}_{cf} = \gamma_{cf}\,\frac{\mathcal{F}}{|\mathcal{F}_c - \mathcal{F}_f|} = \left(\frac{\hbar^2}{2\mu}\left|\frac{\mathcal{F}_c\mathcal{F}_f}{\mathcal{F}_c-\mathcal{F}_f}\right|^2\right)^{1/3}. \tag{36}$$

The damping factor $\exp(-2\Gamma\tau)$ on the right-hand side of Eq. (35) shows that the time τ of propagation on the core-excited potential surface $U_c(R)$,

$$\tau \simeq \int_{a(R_0)}^{R_{cf}} \frac{dR}{v(R)}, \quad v(R) = \left(\frac{2}{\mu}[\omega - \omega_{c0}(R)]\right)^{1/2}, \tag{37}$$

to the crossing point R_{cf} where the emission transition takes place, cannot exceed the lifetime Γ^{-1} of the core-excited state. This estimation agrees with another, deeper, treatment of the damping factor given in Sec. II A [here see Eqs. (13) and (14)]. Equation (37) admits a simple estimation of the propagation time, $\tau \sim (R_{cf}-R_0)/v$, with the characteristic velocity $v \sim \sqrt{2\Delta U/\mu}$ and of the shift of the potential, $\Delta U = U_c(R_0) - U_c(R_{cf})$, during this propagation. The fundamental role played by the interference between different intermediate continuum states in forming the damping factor $\exp(-2\Gamma\tau)$ was shown earlier in Sec. II A.

Comparison of Eqs. (31) and (35) (see also Figs. 3 and 4). shows that the contribution of the ''molecular'' region (35) in the RXS cross section is $(\Gamma/\gamma_{cf})^2$ times smaller than the contribution (31) of the ''dissociative'' region. The factor

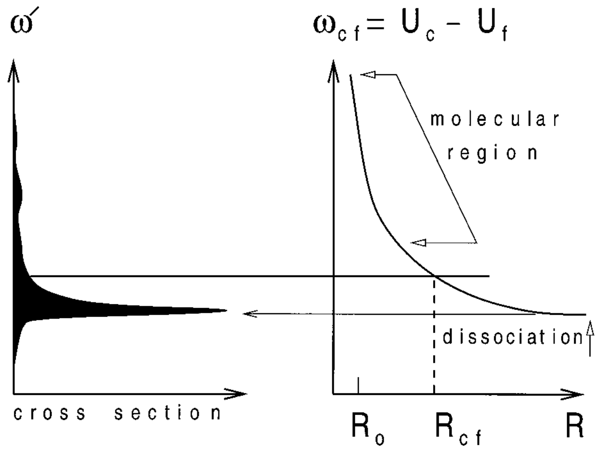

FIG. 4. Qualitative dependence of the spectral shape of the continuum-continuum RXS cross section on the emission frequency ω'. When the lifetime broadening is sufficiently small, the decay transitions in the molecular region form the wing of the spectral band with weak intensity in comparison with the narrow resonance caused by decay transition in the dissociative region. According to Eqs. (35) and (38), the spectral shape of the wing has an oscillatory character.

$(\Gamma/\gamma_{cf})^2$ increases only when the crossing point R_{cf} tends to the dissociative region where γ_{cf} decreases according to Eq. (24).

If the frequency ω of the initial photon is tuned to the absorption maximum ($\Delta\omega=0$), the RXS cross section (35) becomes proportional to $\mathrm{Ai}^2[-(\delta/\overline{\gamma_{cf}})]$. The factor $(\delta/\overline{\gamma_{cf}})$ is large for large R_{cf}. Taking into account the asymptotic form of the Airy function [35,36], we have the following expression for the cross section (35):

$$\sigma_{\mathrm{cc}}(\omega',\omega)=\sigma\,\frac{\Gamma}{\gamma_{cf}^2}\,\frac{\mathcal{F}_{f0}\mathcal{F}_f}{\mathcal{F}_{c0}\mathcal{F}_c}\,e^{(-(a_{c0}/a_0)^2)}e^{-2\Gamma\tau}\times\left(\frac{\overline{\gamma_{cf}}}{\delta}\right)^{1/2}\sin^2\left[\frac{2}{3}\left(\frac{\delta}{\overline{\gamma_{cf}}}\right)^{3/2}+\frac{\pi}{4}\right]. \quad (38)$$

According to Eq. (33) the turning point $R_{cf}=\omega_{cf}^{-1}(\omega')$ depends on the emission frequency. Thus $\delta=U_c(R_0)-U_c(R_{cf})$ is also a function of ω'. Expression (38) shows that the Airy function leads to slowly damped oscillations of the cross section in the "molecular" region ($R_0<R_{cf}<\infty$). This slow damping $\propto\sqrt{\overline{\gamma_{cf}}/\delta}$ is halted in the region close to the dissociation where the factor $(\Gamma/\gamma_{cf})^2$ starts to increase, and the RXS cross section is described by Eq. (31). Cross sections (35) and (38) play the role of the background for the resonance contribution (31) in the dissociative region, as illustrated in Fig. 4.

To clarify the frequency dependence of the cross section (38), let us consider the power potentials $U_i(R)=U_i(\infty)+\beta_i/R^n$. The solution of Eq. (33) then leads to the crossing point

$$R_{cf}=\left(\frac{\beta_c-\beta_f}{\Delta}\right)^{1/n},\quad \Delta=\omega'-\omega_{cf}(\infty), \quad (39)$$

and to the following frequency dependence of the parameters in Eq. (38):

$$\frac{\delta}{\overline{\gamma_{cf}}}\propto(\Delta\omega_\infty-\Delta)\Delta^{-2/3[1+(1/n)]},\quad \frac{\mathcal{F}_f}{\mathcal{F}_c\gamma_{cf}^2}\propto\Delta^{-4/3[1+(1/n)]}, \quad (40)$$

where $\Delta\omega_\infty=\omega_{cf}(R_0)-\omega_{cf}(\infty)$.

D. Spectral features

1. Continuum-bound and continuum-continuum decay channels

We first consider the common case when the intermediate vibrational states are continuous (Fig. 1). This occurs when the core-excited state has a strict repulsive, dissociative, potential, or when the excitation takes place above the dissociation threshold. A typical example is the H_2S molecule. As shown in Ref. [10], this molecule has dissociative potentials for the $^1A_1(3a_1^{-1}6a_1^1)$ and $^1B_2(3a_1^{-1}3b_2^1)$ $2p$ core-excited states. The core-excited state can then decay through the two continuum-continuum and continuum-bound channels. The total cross section σ given by Eq. (5) will then be the sum of the two partial cross sections σ_{cb} and σ_{cc}.

We first consider the continuum-continuum decay channel. The cross sections for this channel, (28), (31), and (35) have no δ singularity due to the continuous nature of the final state. The spectral width $\tilde{\gamma}$ of the continuum-continuum cross sections $\sigma_{\mathrm{cc}}(\omega',\omega)$ [(28), (31), and (35)] is defined by the width of the most narrow factor: $\tilde{\gamma}=\gamma_f$ in the first limiting case (26), $\tilde{\gamma}=\min(\gamma_c,\Gamma)$ in the second limiting case (29), and $\tilde{\gamma}=\min(\gamma_c,\gamma_{cf})$ in the third case (34). Contrary to Γ and γ_c (19), the width γ_{cf} of the continuum-continuum FC factors strongly depends on the frequences ω and ω' and on the shape of the potentials $U_c(R)$ and $U_f(R)$. Indeed, γ_{cf} can be large only in the "molecular" region $R_{cf}\sim R_0$, where the slopes $\mathcal{F}_c$ and $\mathcal{F}_f$ can differ strongly. The x-ray emission intensity will have an oscillatory dependence on ω' (35) until condition (34) is valid. When the frequency ω' is tuned to the dissociative region [see Eq. (33)], both $\mathcal{F}_c$ and $\mathcal{F}_f$ tend to zero, as a result γ_{cf} also tends to zero. Thus for emission in the dissociative region the RXS spectral shape (29) will be that of a single atomiclike resonance (31).

In the continuum-bound decay channel the cross section σ_{cb} will have a sharp frequency dependence, as described by the δ function (5). The RXS scattering amplitude $F_{f(m)}$ of this channel, defined by Eq. (7), depends on two different FC factors, (19) and (20), with different vibrational parameters. Equations (19) and (20) show that the RXS amplitude (7) is a convolution of Lorentzian and Gaussian functions with the widths Γ, γ_c, and $\tilde{\gamma}_c$. So the cross section $\sigma_{\mathrm{cb}}(\omega',\omega)$ is described by the Voigt contour for the given relation between these widths.

According to Eqs. (7), (19), and (20), the frequency dependence of $\overline{\sigma_{\mathrm{cb}}}(\omega',\omega_c)$ takes the following remarkable form when $\Gamma\ll\gamma_c,\tilde{\gamma}_c$:

$$\overline{\sigma_{\mathrm{cb}}}(\omega',\omega_c)=\overline{\sigma}\sum_m\Phi(\omega-\omega_c,\gamma)(\varphi_0(x)\varphi_m^f(\tilde{x}))^2, \quad (41)$$

with

$$\omega=\omega'+\omega_{f0}(R_0^f)+\omega_m, \quad \overline{\sigma}=\frac{\omega'}{\omega}(2\pi\mu VQ)^2(a_{c0}\widetilde{a}_{c0})^3,$$

$$x=-\frac{1}{\mathcal{F}_{c0}}[\omega'-(U_c(R_0)-U_f(R_0^f))+\omega_m+\mathcal{F}_{c0}a_{c0}], \tag{42}$$

$$\widetilde{x}=-\frac{1}{\widetilde{\mathcal{F}}_{c0}}[(\omega'-\omega_{cf}(R_0^f))+\omega_m+\widetilde{\mathcal{F}}_{c0}\widetilde{a}_{c0}].$$

The vibrational energy of the final state ω_m is equal to $(m+1/2)\widetilde{\omega}_0$ in the harmonic approximation. In the opposite limiting case $\Gamma \gg \gamma_c, \widetilde{\gamma}_c$ the scattering cross section is described by the Lorentzian according to the short-lifetime limit (27) and the overlap integral between $\varphi_m^f(R)$ and $\varphi_0(R)$. The effective coordinates x and $\widetilde{x}$ of absorption and emission transitions depend on the emission frequency ω'. The square of the vibrational wave functions in Eq. (41) gives the spectral features with the widths $\gamma_c=\mathcal{F}_{c0}a_0$ and $\widetilde{\gamma}_c=\widetilde{\mathcal{F}}_{c0}\widetilde{a}_0$ since the bound-state wave functions $\varphi_m^f(R)$ and $\varphi_0(R)$ depend on $\widetilde{x}$ and x through the dimensionless ratios $\widetilde{x}/\widetilde{a}_0$ and x/a_0. It is important to remember that $\widetilde{x}$ is the classical turning point [see Eq. (19)].

The spectral shape of the total cross sections (4) and (5) in the considered case is defined by two resonant features with qualitatively different frequency scales. The spectral width of $\overline{\sigma}_{\rm cb}$ is equal to zero when the width of the spectral function is negligibly small. The continuum-continuum contribution $\overline{\sigma}_{\rm cc}$ in this case plays the role of a background with the width $\widetilde{\gamma}$. Let us briefly analyze the main features of the cross section $\overline{\sigma(\omega',\omega_c)}$ (4) in the dissociative limits (29) and (31) convoluted with the spectral function $\Phi(\omega-\omega_c,\gamma)$ of incoming x-ray radiation. The spectral width of $\overline{\sigma}_{\rm cb}$ is equal to the spectral width γ of Φ when $\gamma \ll \gamma_c, \widetilde{\gamma}_c$, and is equal to $\min(\gamma_c,\widetilde{\gamma}_c)$ in the opposite limit. $\overline{\sigma}_{\rm cc}$ [(4) and (31)] has a qualitatively different dependence on γ. When $\gamma_c \gg \Gamma$ the spectral width of $\overline{\sigma}_{\rm cc}$ in the dissociative region is equal to the lifetime broadening Γ and does not depend on γ. The corresponding γ dependence appears if $\gamma_c \leqslant \Gamma$. In the molecular region $\overline{\sigma}_{\rm cc}$ [(35) and (38)] forms an oscillatory background with the characteristic energy scale of oscillations $\gamma_{cf}\sim 1$ eV.

We would like to direct attention to the spectral features demonstrated by Eq. (41). One can see from this equation that the spectral shape of the RXS cross section is proportional to the square of the final-state vibrational wave function. In the harmonic approximation this function is proportional to the Hermite polynomial $(\varphi_m^f(x)\propto \exp[-(x/\widetilde{a}_0)^2/2]H_m(x/\widetilde{a}_0))$. Moreover, the partial RXS cross section connected with a certain final vibrational state m is equal to zero for the m nodes (zeros) of the vibrational wave function. So we arrive at the important conclusion that resonant x-ray scattering under transitions between continuum and bound states allows the direct measurement of the vibrational wave function.

2. Bound-bound and bound-continuum decay channels

Now let us consider the x-ray excitation below the dissociation threshold (Fig. 4). In this case the intermediate vibrational states φ_m^c are bound, allowing for only bound-bound and bound-continuum decay channels. In the general case of several excited intermediate vibrational states, the scattering channels will interfere through these discrete states [29,30,26,31]. Now, the total cross section is the sum of bound-bound and bound-continuum cross sections; $\sigma(\omega',\omega)=\sigma_{\rm bb}(\omega',\omega)+\sigma_{\rm bc}(\omega',\omega)$. The properties of $\sigma_{\rm bb}(\omega',\omega)$ proportional to the δ function have been investigated earlier [29–31] and will therefore not be discussed here.

In accordance with Eqs. (7) and (20) the contribution of the bound-continuum decay channel to the total RXS cross section is equal to

$$\sigma_{bc}(\omega',\omega)=\left|\sum_m q_m \frac{\varphi_m^c(x)}{\omega-\omega_{c0}(R_0^c)-\omega_m+i\Gamma}\right|^2 \tag{43}$$

when $\Gamma \ll \gamma_f, \widetilde{\gamma}_f$. Here

$$x=\frac{1}{\widetilde{\mathcal{F}}_{f0}}(\omega-\omega'-\omega_{f0}(R_0^c)+\widetilde{\mathcal{F}}_{f0}\widetilde{a}_0),$$

$$q_m=\left(2\mu\widetilde{a}_{f0}^3\frac{\omega'}{\omega}\right)^{1/2}VQ\langle\varphi_m^c|\varphi_0\rangle. \tag{44}$$

$\widetilde{a}_0=\sqrt{\hbar/\mu\widetilde{\omega}_0}$, ω_m is the vibrational energy of the core excited state [$\omega_m=(m+1/2)\widetilde{\omega}_0$ in the harmonic approximation]. All other quantities are calculated at the equilibrium point of the core-excited state, and they are defined by Eqs. (19) and (20) after the replacement $c\to f$. Since the final state is continuous, this cross section has no δ singularity, contrary to $\sigma_{\rm bb}(\omega',\omega)$. It is remarkable that the dependence of the cross section (43) on the emission frequency ω' copies the space distribution of the vibrational wave function $\varphi_m^c(x)$. Indeed, if $\Gamma<\widetilde{\omega}_0$ one can tune the frequency into an exact resonance with some vibrational state m. In this case the RXS cross section (43) simply becomes

$$\sigma_{bc}(\omega',\omega)\propto(\varphi_m^c(x))^2. \tag{45}$$

This equation shows how the vibrational wave function can be mapped, and that the cross section is equal to zero in the m points where $\varphi_m^c(x)$ is equal to zero. Equation (45) leads to the simple geometrical consideration given in Fig. 5. This consideration is based on the physical meaning of x (44) as the classical turning point for propagation on the potential surface U_f of the final dissociative state [see Eqs. (19) and (20)]. According to this physical meaning the spectral shape of the RXS cross section reflects the square of the vibrational wave function $(\varphi_m^c(x))^2$ of the core-excited state by the linearized potential of the final state (Fig. 5). This geometrical interpretation of Eq. (20) reminds one of the common geometrical approach to estimating spectral linewidths in photoelectron spectra [38,37]. It is important to note that Eq. (45) and its geometrical interpretation [Fig. 5(a)] are based on the linear approximation of the potential U_f near R_0^c. Thus only in the case of such a linear potential the mapping $\sigma_{\rm bc}(\omega',\omega)\propto(\varphi_m^c(x))^2$ is linear [see Fig. 5(a)]. In the general case of a nonlinear potential the mapping is evidently nonlinear [see Fig. 5(b)], and the application of the reflection method will not produce a direct copy of the squared wave

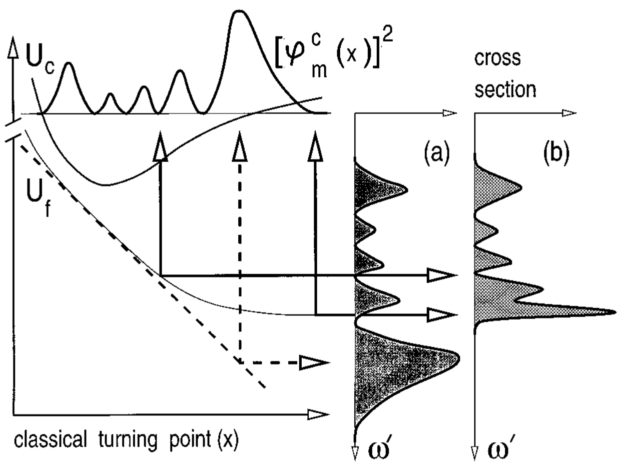

FIG. 5. Geometrical illustration of the proportionality of the bound-continuum RXS cross section $\sigma_{bc}(\omega',\omega)$ (45) to the square of the vibrational wave function $\varphi^c_m(x)$ of the core-excited state at the classical turning point x (44). The linear approximation of the final-state potential U_f is depicted with a thick dashed line; the exact potential U_f is depicted with a thin solid line. The cross sections are obtained by reflection on (a) a linear potential, and (b) a nonlinear potential.

function, as given by Eq. (45), but a deformation of this wave function depending on the particular shape of the potential asymptot.

Now let us briefly discuss the frequency scales of the total cross section $\tilde{\sigma}(\omega',\omega)$ convoluted with the spectral function Φ (4). If $\gamma \ll \Gamma$ the width of $\overline{\sigma_{\rm bb}}$ is defined only by the width γ of the spectral function Φ, and can be obtained to be very narrow, while the width of the bound-continuum cross section $\overline{\sigma_{\rm bc}}$ cannot be obtained to be smaller than the width $\overline{\gamma}$ of the product of the Lorentzian and Gaussian functions; $\overline{\gamma}=\min(\Gamma,\tilde{\gamma}_f)$. The qualitative dependence of the spectral linewidth given by the continuum part $\overline{\sigma_{\rm bc}}$ of the cross section goes as follows: The width of $\overline{\sigma_{\rm bc}}$ for a single vibrational level m decreases approximately from $(\gamma+\overline{\gamma})$ to $\overline{\gamma}$ when the width γ of the spectral function Φ decreases. When $\gamma \ll \overline{\gamma}$ the spectral shape of the total cross section for a single intermediate vibrational level m is represented by a narrow band $\overline{\sigma_{\rm bb}}$ (4) with the width γ on top of a background comprising a broad continuum contribution $\overline{\sigma_{\rm bc}}$ [(43), (45), and (4)] with the width $\overline{\gamma}=\min(\Gamma,\tilde{\gamma}_f)$.

3. Bound-continuum and continuum-continuum decay channels

In some cases, as for example for HCl [41], the x-ray photons core excite the molecule to a point of the upper potential surface which is close to the dissociation threshold (Fig. 1). In this case both bound and continuous vibrational states of the intermediate state are populated (Fig. 1). Here let us consider only a repulsive final state, as for instance reached by nonradiative RXS of HCl from the $3\sigma^1\sigma^{*1}$ ($^1\Sigma^+$) intermediate state [41]. The total cross section for the two decay channels, the bound-continuum and continuum-continuum decay channels, now becomes the sum of the above defined bound-continuum $\sigma_{\rm bc}$ (45) and continuum-continuum $\sigma_{\rm cc}$ [(28), (31), and (35)] partial cross sections: $\sigma(\omega',\omega)=\sigma_{\rm bc}(\omega',\omega)+\sigma_{\rm cc}(\omega',\omega)$]. Due to the continuous nature of the final state, both of these partial cross sections lack δ singularity, and the widths of the corresponding resonances cannot be made small by narrowing the spectral width of exciting radiation (lack of resonance narrowing). As was shown above, the spectral width of $\sigma_{\rm bc}$ is equal to $\overline{\gamma}=\min(\Gamma,\tilde{\gamma}_f)$, and is defined by the lifetime broadening and by the spectral width of the bound-continuum FC factor. Depending on the circumstance (as described above) the spectral width $\tilde{\gamma}$ of $\sigma_{\rm cc}$ is defined by three characteristic factors: the lifetime broadening (Γ), the width of the bound-continuum FC factors (γ_c or γ_f), and the width of the continuum-continuum FC factors (γ_{cf}).

III. RESONANT X-RAY SCATTERING INVOLVING DISSOCIATIVE STATES. TIME-DEPENDENT THEORY

A. Time-dependent representation of the RXS cross section

To carry through a time-dependent formulation of the RXS cross sections, let us restart from the generalized Kramers-Heisenberg formulas for the radiative and nonradiative RXS cross section, Eqs. (1), (2), and (3). Taking into account that $E_c,|c\rangle$ and $E_f,|f\rangle$ are eigenvalues and eigenfunctions of the Hamiltonians H_c and H_f of the core-excited and final states, one can express the denominator Δ and δ functions in Eqs. (2) and (3) as an integral over time:

$$\frac{1}{\omega-\omega_{c0}+i\Gamma}\rightarrow\frac{1}{\omega+E_0-H_c+i\Gamma}=i\int_0^\infty dt\; e^{i(\omega+E_0-H_c)t-\Gamma t}. \tag{46}$$

The RIXS cross section and the REXS amplitude now read

$$\sigma^{\rm RIXS}(\omega',\omega)=\frac{\omega'}{\omega\pi}\times{\rm Im}\int_0^\infty dt\int_0^\infty d\tau\int_0^\infty dt_1 e^{\theta}\langle 0|V^+G_c^-(-t)\times Q_f^+G^+(\tau)QG_c^+(t_1)V|0\rangle, \tag{47}$$

$$F_0=\int_0^\infty dt\;\exp[i(\omega+E_0)-\Gamma t]\langle 0|V'G_c^+(t)V|0\rangle,$$

where

$$\theta=i\phi-\Gamma(t+t_1)-\gamma_0\tau,$$

$$\phi=(\omega+E_0)(t_1-t)+(\omega-\omega'+E_0)\tau. \tag{48}$$

The retarded and advanced Green's functions, $G_i^+(t)$ and $G_i^-(-t)=[G_i^+(t)]^+$, here introduced ($i=c,f$), read [42]

$$G_i^\pm(\pm t)=\begin{cases}\mp ie^{\mp iH_it} & \text{if } t>0\\ 0 & \text{if } t<0.\end{cases} \tag{49}$$

$G_i^+(t)$ describes the propagation of the wave packet subject to the Hamiltonian H_i forward in time, and $G_i^-(t)$ the same backward in time. A time-dependent representation for the RIXS cross section, Eqs. (47) and (49), was presented in Ref. [29]; a more recent representation of $\sigma^{\rm RXS}$ has been given by Cederbaum and Tarantelli [32] using the concept of wave packets accompanying the excitation to a decaying electronic state and the subsequent decay to final electronic states. A time-dependent wave packet approach of Raman scattering was developed earlier by Heller and co-workers [43,44]. The present time-dependent theory generalizes the theory of Cederbaum and Tarantelli [32], which is applicable only to broadband excitation, and gives different results, for example, if the final state is bound or short lived.

It necessary to note that Hamiltonians H_c and H_f are identical and equal to the total molecular Hamiltonian in strict theory. Let us focus on RXS features influenced by the nuclear dynamics in both the decaying $|c\rangle$ and final $|f\rangle$ states. In this case H_c and H_f are the Hamiltonians describing the nuclear motion in the core-excited and final state and do not coincide. Electronic matrix elements V and Q for absorption and decay transitions are functions of the nuclear coordinates of the target.

The wave-packet representation allows us to rewrite Eq. (47) in a more compact form after transition to different time variables $(t\rightarrow t, t_1\rightarrow t+T)$

$$\sigma^{\mathrm{RIXS}}(\omega',\omega)=-q\ \mathrm{Re}\int_0^\infty dt\int_0^\infty dT\int_0^\infty d\tau\ e^{i\phi}\sigma_\tau(t,t+T),$$
$$F_0=-i\langle 0|\psi_{0c}(0,0)\rangle\int_0^\infty dt\ e^{i(\omega+E_0)t}F(t), \tag{50}$$

where $q=\langle 0|V^+Q^+QV|0\rangle\omega'/(\pi\omega)$. This equation is a generalization of the theory in Ref. [32], taking account of the energy conservation law (δ-energy function) for the RXS process. With our time variables the phase ϕ is equal to $\phi=(\omega+E_0)T+(\omega-\omega'+E_0)\tau$. The autocorrelation functions introduced here are defined by

$$\sigma_\tau(t,t+T)=qe^{-\gamma_0\tau}e^{-\Gamma(2t+T)}\frac{\langle\psi_{fc}(0,t)|\psi_{fc}(\tau,t+T)\rangle}{\langle\psi_{fc}(0,0)|\psi_{fc}(0,0)\rangle},$$
$$F(t)=e^{-\Gamma t}\frac{\langle 0|\psi_{0c}(0,t)\rangle}{\langle 0|\psi_{0c}(0,0)\rangle}. \tag{51}$$

These functions are normalized to unity [$\sigma_0(0,0)=1$, $F(0)=1$] and $\langle\psi_{fc}(0,0)|\psi_{fc}(0,0)\rangle=\langle 0|V^+Q^+QV|0\rangle$ and $\langle 0|\psi_{0c}(0,0)\rangle=\langle 0|V'V|0\rangle$. The wave packets

$$\psi_c(t)=iG_c^+(t)\psi_c(0),\quad \psi_c(0)=V|0\rangle,$$
$$\psi_{fc}(\tau,t)=iG_f^+(\tau)Q\psi_c(t),\quad \psi_{0c}(0,t)=V'\psi_c(t) \tag{52}$$

have the following meaning. At time $t=0$ the initial vibrational state $|0\rangle$ is excited at rate V to the intermediate nuclear state, and arrives there as a wave packet $\psi_c(0)=V|0\rangle$. The wave packet $\psi_c(t)=iG_c^+(t)\psi_c(0)$ propagates on the potential surface $U_c(R)$ of the core-excited state $|c\rangle$; it can be expressed through the wave packet $\psi_c(0)$ of the initial time $t=0$ with help of the propagator $G_c^+(t)$. At some time t this wave packet decays with the rate Q to the final state $|f\rangle$, at which moment the wave packet $\psi_{fc}(0,t)=Q\psi_c(t)$ appears in the final state. The propagation of this wave packet on the final-state potential surface $U_f(R)$ is governed by the retarded Green's function $G_f^+(\tau)$. After the time τ the initial wave packet $\psi_{fc}(0,t)$ evolves to the wave packet $\psi_{fc}(\tau,t)=iG_f^+(\tau)\psi_{fc}(0,t)$ (52). During the time of evolution the population of the core-excited state $|c\rangle$ decreases due to the finite lifetime Γ^{-1} of this state. The corresponding decrease of amplitudes of the wave packets $\psi_{fc}(0,t)$ and $\psi_{fc}(\tau,t+T)$ (51) is reflected in the autocorrelation function $\sigma_\tau(t,t+T)$ (51) by the decaying factor $\exp[-\Gamma(2t+T)]$. The final state $|f\rangle$ has also a finite lifetime γ_0^{-1}. Therefore, the amplitude of the wave packet $\psi_{fc}(\tau,t+T)$ propagated during the time τ on the potential surface of the final state $|f\rangle$ decreases as $\exp(-\gamma_0\tau)$ (51).

In accordance with the expression for the autocorrelation function $\sigma_\tau(t,t+T)$ (51), the final state $|f\rangle$ can be reached under inelastic scattering by two different ways involving two potentials. These ways differ by the times t and $t+T$ of decay transition $c\rightarrow f$ to the final state, and by the different times lapses 0 and τ of propagation on the final-state potential surface $U_f(R)$ (see the lower panel of Fig. 2). The first path is given by the absorption transition to state $|c\rangle$ at the initial time $t=0$, by the propagation on the potential surface $U_c(R)$, and by the decay transition $c\rightarrow f$ to the final state at time t. This path leads to the final wave packet $\psi_{fc}(0,t)$ (Fig. 2). The second path is given by core excitation to the state $|c\rangle$ at $t=0$ with forthcoming propagation on the potential surface $U_c(R)$, by the decay transition $c\rightarrow f$ at time $t+T$, and by the propagation in the field of the potential $U_f(R)$ during the time τ (Fig. 2). At the end of this path the final wave packet equals $\psi_{fc}(\tau,t+T)$. The cross section (50) of inelastic scattering is the half-Fourier transform of the autocorrelation function (51) which correlates the wave packets $\psi_{fc}(0,t)$ and $\psi_{fc}(\tau,t+T)$ at the same point but at different times.

The wave packet representation, Eqs. (50) and (51), allows us to give an alternative treatment of the interference effects in comparison with the time-independent theory. The autocorrelation function $\sigma_\tau(t,t+T)$ describes the time coherence or interference of time-shifted wave packets (see the lower panel in Fig. 2). We will refer to this interference of time-shifted wave packets as to t coherence or t interference. The decay of core-excited state $|c\rangle$ destroys the t coherence. The multiplier $\exp[-\Gamma(2t+T)]$ in Eq. (51) shows that the corresponding coherence time, estimated as effective retardation time T, does not exceed the lifetime of the intermediate state

$$T\lesssim\frac{1}{\Gamma}. \tag{53}$$

The notion of interference of RIXS is different in the time-independent theory [29–31]; the interference between RXS channels is defined by the energies E_c of the intermediate states $|c\rangle$ [see Eq. (2) and the upper panel in Fig. 2]. We will refer to this interference as E interference or E coherence. As known from the time-independent theory of RIXS [29–31], the E interference between two different scattering channels is large if the energy gap $\Delta E=E_c-E_c'$ between different intermediate states is smaller than or comparable with the lifetime broadening

$$\Delta E\lesssim\Gamma. \tag{54}$$

In other words, the length of coherence in E space is defined by the lifetime broadening Γ, while the length of coherence in the t representation or the coherence time is restricted by Γ^{-1} (53). Thus Eqs. (53) and (54) show that when E interference or E coherence is large ($\Gamma\to\infty$), the t interference or t coherence is small, and vice versa. This follows indirectly also from the uncertainty principle.

Contrary to Cederbaum and Tarantelli [32], Eqs. (47) and (50) contain an additional integration over time τ. This third integral is of principal importance as it leads to the Δ singularity of the RXS cross section (2) caused by the energy conservation law. The amplitude of the elastic scattering F_0 (51) is the half-Fourier transform of the overlap of the ground-state vibrational state $|0\rangle$ and the wave packet $\psi_{0c}(0,t)$ (52) [43]. The physical meaning of this wave packet is the same as that of the wave packet discussed above, $\psi_{fc}(0,t)$, if here we replace the index f by the index 0 of the ground state.

One can also adopt a Condon approximation in which V, V', and Q are assumed to be constant. The RIXS cross section and REXS amplitude (47) are then simplified considerably because V, V', and Q may be extracted from all integrals. To rewrite Eqs. (47), (50), and (52) in the Condon approximation, we need to use $V=V'=Q=1$, $\langle\psi_{fc}(0,0)|\psi_{fc}(0,0)\rangle=1$, $\langle 0|\psi_{0c}(0,0)\rangle=1$, and $q=|VQ|^2\omega'/(\pi\omega)$, and we have to introduce the multiplier $V'V$ at the right-hand side of the expression for $F(t)$ (51).

B. Time-dependent analysis of the RXS amplitude

To analyze the dynamics of the propagation of wave packets in coordinate space, the language of scattering amplitudes is appropriate. The RXS scattering amplitude (2) can be written in terms of the time-independent Green's function broadened by Γ as

$$G_E^+=\frac{1}{E-H_c+i\Gamma}=\int_0^\infty dt\; e^{(iE-\Gamma)t}G_c^+(t), \tag{55}$$

or in terms of the time-dependent Green's function as

$$F_f=\langle f|QG_E^+V|0\rangle=\int_0^\infty dt\; e^{(iE-\Gamma)t}\langle f|QG_c^+(t)V|0\rangle. \tag{56}$$

Here we use the Green's functions G_E^+ and $G_c^+(t)$ (49) defined by the Hamiltonian $H_c'=H_c-U_0(R_0)$, the potential $U_c'(R)=U_c(R)-U_c(R_0)$, and the energy $E=\omega+E_0-U_c(R_0)$ shifted by $U_c(R_0)$. Comparing the right-hand side of Eq. (56) and the definition of the wave packet $\psi_{fc}(0,t)$ (52), we find

$$\begin{aligned}F_f&=-i\int_0^\infty dt\; e^{(iE-\Gamma)t}\langle f|\psi_{fc}(0,t)\rangle\\&=-i\int_{-\infty}^\infty dx\;\psi_f^*(x)\left\{\int_0^\infty dt\; e^{(iE-\Gamma)t}\psi_{fc}(0,t;x)\right\},\end{aligned} \tag{57}$$

where $\psi_{fc}(0,t;x)$ is the wave packet in the coordinate representation. This equation is useful for qualitative analysis of RXS under transitions between dissociative states. Let us assume the Condon approximation for simplicity, and extract V and Q from the integral in Eq. (57). In this case the wave packet $\psi_{fc}(0,t;x)$ coincides with the solution of the time-dependent Schrödinger equation in the potential of the core-excited state $U_c(R)$ with initial wave function $\varphi_0(x)$ (16). One can understand the main features of a wave-packet propagation if one looks for the solution of this problem with a linear potential $U_c'(R)=U_c(R)-U_c(R_0)=Fx$ ($F=F_c=\text{const}>0$, $x=R-R_0$) [45],

$$\psi_{fc}(0,t;x)=\left(\frac{1}{\pi a(t)^2}\right)^{1/4}\exp\left[-\frac{1}{2}\left(\frac{x-x_c(t)}{a(t)}\right)^2\alpha+i\beta\right], \tag{58}$$

where

$$x_c(t)=Ft^2/2\mu,\quad a(t)=a_0\left[1+\left(\frac{t}{\tau_0}\right)^2\right]^{1/2},\quad \tau_0=\frac{\mu a_0^2}{\hbar}, \tag{59}$$

and $\alpha=1-it/\tau_0$, $\beta=Ft(x-Ft^2/6\mu)$. Equation (58) shows that the probability density distribution remains Gaussian-like just as the ground-state distribution $\varphi_0^2(x)$ (16) and that the center of gravity $x_c(t)$ of the wave packet moves according to the law of classical mechanics with a uniform acceleration F/μ. The width of the packet $a(t)$ which originally was a_0 increases with time according to Eq. (59). The characteristic time for the wave-packet spread is τ_0. The physical reason for this spread is the different velocities p/μ of motion of different Fourier components $\exp(ipx)$ of the wave packet. It also follows indirectly from the uncertainty of momentum $\Delta p\sim 1/a$ caused by the finite dimensions of the wave packet. In the dissociation region $E>U_c(\infty)-U_c(R_0)$, one can also expect in the case of a general potential that the center of mass $x_c(t)$ of the wave packet moves according to the law of classical mechanics $\mu\ddot{x}_c=F(x_c)$. The time dependence of the spread $a(t)$ (59) of the wave packet depends in the general case on the shape of $\varphi_0(x)$ and on the potential. Contrary to the case of linear potentials, the general case is complicated by inhomogeneities of the potential. Equations (52) and (57) show that during the propagation on the intermediate state potential surface $U_c(R)$ the wave packet continuously decays to the final electronic state. The factor $\exp(-\Gamma t)$ (57) describes the decrease of the wave-packet amplitude caused by the decay-induced decrease of the core-excited state population. Thus the decay transitions $c\to f$ can take place only when the time of decay transitions does not exceed the lifetime and, as a consequence, when the coordinate for the center of mass of the wave packet does not exceed the distance covered by the wave packet during this lifetime,

$$0\le t\le\frac{1}{\Gamma},\quad x_c\le\frac{v_c}{\Gamma}. \tag{60}$$

Here $v_c\sim\sqrt{\Delta V/\mu}$ is the characteristic velocity of the wave-packet propagation, and $\Delta V=U_c(R_0)-U_c(R_0+x_c)$ is the change of the intermediate-state potential under propagation of the wave packet. To obtain $x_c=Ft^2/2\mu$ (59), one can estimate the slope as $F\sim\Delta V/x_c$. It is relevant to note that the center of gravity x_c and the crossing point R_{cf} cannot be equal. These quantities have different magnitudes and different physical meanings. Indeed, x_c is the time-dependent character of the wave packet or coherent superposition of the infinite set of wave functions, while the crossing point R_{cf} is the characteristic of the FC factor between two stationary wave functions. However, these two quantities also have a common property, namely, that they cannot exceed v_c/Γ. In Sec. III B1 we examine the two important limiting cases of short- and long-lived intermediate states.

1. Short-lived core-excited states

When the lifetime Γ^{-1} of the core-excited state is small,

$$\frac{v_c}{\Gamma} \leqslant a_0, \tag{61}$$

the nuclei have no time move far away from the equilibrium point R_0 and the wave packet does not spread. This means that the wave packet $\psi_{fc}(0,t)$ is a smoother function over time than $\exp(-\Gamma t)$, and that one can extract $\langle f|\psi_{fc}(0,t)\rangle$ from the integral (57) at point $t=0$. Because $G^+(0)=-i$ and, as a result, $\psi_{fc}(0,0)\rangle = QV|0\rangle$, we have [31]

$$F_f = \frac{1}{E+i\Gamma}\langle f|QV|0\rangle \simeq \frac{QV}{E+i\Gamma}\langle f|0\rangle. \tag{62}$$

One can see from the latter expression written in the Condon approximation that inelastic ($f\neq 0$) and elastic ($f=0$) scattering amplitudes are defined by a projection of the final vibrational state $|f\rangle$ on the ground vibrational state $|0\rangle$. The FC factor $\langle f|0\rangle$ is defined by a narrow region close to R_0 with the width a_0 due to strong localization of the ground-state vibrational function $|0\rangle$. This is the case for a vertical transition because the initial wave packet $|0\rangle$ has no time to spread during the lifetime of the core-excited state. It is of interest to note that the intermediate vibrational states $|c\rangle$ do not take part in RXS in the short-time limit [see Eq. (62)]. The amplitude of elastic scattering is simplified considerably by the Condon approximation

$$F_0 = \frac{VV'}{E+i\Gamma} \tag{63}$$

according to $\langle 0|0\rangle = 1$.

2. Long-lived core-excited states

We now consider the opposite long-lived limiting case when the lifetime broadening Γ of the intermediate state (34) is narrow in comparison with the widths γ_c (19) and γ_{cf} (24) of absorption and emission FC factors. With aid of the identity $1/(x\pm i0) = \mp i\pi\delta(x) + \wp(1/x)$ and the FC rule, we obtain from Eqs. (2) and (3)

$$\begin{aligned} F_f &= -VQ\left(i\pi\langle \varphi^f_{E_f}|\varphi^c_E\rangle\langle\varphi^c_E|\varphi_0\rangle \right.\\ &\quad \left. +\wp\int dE_c\,\frac{\langle\varphi^f_{E_f}|\varphi^c_{E_c}\rangle\langle\varphi^c_{E_c}|\varphi_0\rangle}{E_c-E}\right), \\ F_0 &= -VV'\left(i\pi\left|\langle\varphi_0|\varphi^c_E\rangle\right|^2 + \mathfrak{p}\int dE_c\,\frac{|\langle\varphi_0|\varphi^c_{E_c}\rangle|^2}{E_c-E}\right), \end{aligned} \tag{64}$$

for the RIXS and REXS amplitudes, respectively. The final-state energy E_f is defined by Eq. (6), while $E=\omega+E_0$. So the RIXS and REXS amplitudes are the sums of two contributions. The terms connected with the principal value of the integral over E_c describe the interference between close-lying intermediate continuum states. The long-lived limit for the core-excited dissociative states differs thus qualitatively from the bound core-excited states at the same limit. Let us recall that the interference between different vibrational sublevels of bound core-excited states is absent in this limit [29–31]. Ordinarily, the principal value of the integrals in Eq. (64) is smaller than the main term. We therefore neglected the principal values of the corresponding integrals in Eqs. (35) and (41).

C. Characteristic features of molecular dissociation following x-ray excitation

If the final state $|f\rangle$ is dissociative, the molecule will evidently dissociate independently of the lifetime Γ^{-1} of the core-excited state $|c\rangle$, and independently of the dissociative versus bound character of the core-excited state. The dissociation of state $|f\rangle$ can only be inhibited by decay to a lower-lying bound state, which still often is too slow ($\tau > 10^{-7}$ s) to stop dissociation. As indicated by recent experiments [18,19,46], it is necessary to understand when the RXS spectrum is defined by the molecule in the classical FC region (near the equilibrium internuclear distance R_0 of the ground state) or by the dissociation fragments in the asymptotical region $R \gg R_0$. Let us consider first the case of a continuum intermediate state reached by excitation to a repulsive potential $U_c(R)$ or by excitation above the dissociative threshold $U_c(\infty)$. In the short lifetime limit (61) the molecular fragments have no time to separate and the RXS spectrum is defined by molecular transitions near the equilibrium point R_0. In the opposite limit of large lifetime $v_c/\Gamma \gg R_0$, a molecule has time to propagate into the dissociative region lying far from the equilibrium point R_0. During this propagation the wave packet continuously decays to the final state, emitting x-ray photons and Auger electrons. The RXS spectral shape is formed in accordance with Eq. (64). As follows directly from Eqs. (23) and (24), the continuum-continuum FC factors increase when the slopes $\mathcal{F}_c$ and $\mathcal{F}_f$ are small ($\mathcal{F}_i \to 0$), or when they tend to become equal ($\mathcal{F}_c \to \mathcal{F}_c$). So in the dissociative region where potentials $U_c(R)$ and $U_f(R)$ have small slopes, the FC factors (23) have δ singularity. The emission transition in the dissociative region is thus one taking place in the atomic fragments (atomic transition). The spectral line of this atomiclike transition has the width Γ as was discussed in Sec. II C [see also Eq. (31)]. The emission transitions in the molecular region ($R_{cf} \sim R_0$) where $\mathcal{F}_c \neq \mathcal{F}_c$ gives a background with the width γ_{cf} (24). As shown in Sec. II D, this atomiclike transition has non-Raman behavior and lacks Stokes shifts. This effect was observed recently in the resonant Auger spectra of HCl [20].

IV. SUMMARY

In this work we have presented time-independent and time-dependent theories for radiative and nonradiative resonant x-ray scattering involving dissociative states. We investigated three general types of x-ray scattering channels connecting ground, core-excited, and valence-excited states with bound and dissociative character. We find that the interesting combinations are (1) bound-continuum-bound plus bound-continuum-continuum (bcb+bcc), (2) bound-bound-bound plus bound-bound-continuum (bbb+bbc), and (3) bound-bound-continuum plus bound-continuum-continuum (bbc+bcc) channels. It is shown that these combinations have different limiting factors for the spectral shapes, and that they are different with respect to the relative contributions of the resonant and background parts in the spectra. The spectral shape is defined by the absorption and emission Franck-Condon distributions (with the widths γ_c and/or γ_{cf}), by the lifetime broadening function (width Γ), and by the spectral function of the excitation photons (width γ). In the soft-x-ray region these parameters have typical values of $\gamma_c \sim 1$ eV, $0 < \gamma_{cf} \sim 1$ eV, $\Gamma \sim 0.1$ eV, and $\gamma \sim 0.1$ eV. In the first type of combination (bcb+bcc) the shape of the RXS cross section consists of a narrow line caused by the continuum-bound channel with the width γ, a background with the width equal to the lifetime broadening of the x-ray excited state Γ, and an additional broader background caused by the continuum-continuum channel. The cross section of the bbb+bbc RXS channels is defined by a narrow line caused by the bound-bound channel with width γ and a background caused by the bound-continuum channel with width γ_c. The cross section of the third type of scattering channel (bbc+bcc) is formed by a lifetime-broadened (Γ) resonance and a background with the width γ_c. Contrary to the two previous cases, this last case shows a ''non-Raman'' behavior; the width of the resonance does not depend on the width of the spectral distribution of incoming x-ray photons. Other findings presented in this work can be summarized as follows.

A strong space correlation between excitation and decay is found. This space correlation relates to the finite lifetime of the intermediate core-excited state, more precisely as a characteristic length scale equaling the distance propagated during this lifetime. RXS emission at the internuclear distances beyond the characteristic length is exponentially small.

Selection rules operate for continuum-bound transitions if the slope of the continuum potential is sufficiently small. That is, only transitions to vibrational states with odd quantum numbers are allowed within the harmonic approximation.

The main contribution to the RXS cross section is given by the dissociative region if the lifetime of the core-excited state is sufficiently long. The emission transitions in the molecular region form the wing of the dissociative resonance. The spectral shape of this wing is in general oscillatory with the characteristic energy scale $\gamma_{cf} \sim 1$ eV. It depends strongly on the shapes of the potential surfaces involved in the RXS process. We call attention to detailed experimental investigations of the wings of the RXS spectral lines with the aim of receiving information about potential surfaces of the electronic states involved in the RXS process.

Additional untrivial properties of the RXS cross section for continuum-bound σ_{cb} or bound-continuum σ_{bc} decay transitions have been obtained. Both cross sections are proportional to the square of the wave function of the vibrational states involved in the RXS process. Moreover, the spectral shape of the RXS cross section copies the space distribution of the squared vibrational wave function with the characteristic energy scale $\tilde{\gamma}_c \sim \tilde{\gamma}_f \sim 1$ eV. So an experimental measurement would allow a direct mapping of the vibrational wave function and a reconstruction of the shape of the corresponding molecular potential. Indeed, the zeros of the RXS cross section caused by the nodes of the vibrational wave function allow the assignment of vibrational states.

ACKNOWLEDGMENT

This work was supported by a grant from the Swedish Natural Science Research Council (F.Kh.G.).

[1] R. Mayer, D. W. Lindle, S. H. Southworth, and P. L. Cowan, Phys. Rev. A **43**, 235 (1991).

[2] J. Nordgren, P. Glans, and N. D. Wassdahl, Phys. Scr. **T34**, 100 (1991).

[3] P. Cowan, in *X-ray Resonant Scattering*, edited by G. Materlik K. Fischer, and C. Sparks (North-Holland, Amsterdam, 1994), p. 431.

[4] Y. Ma, N. Wassdahl, P. Skytt, J. Guo, J. Nordgren, J.-E. Rubensson, T. Böske, W. Eberhardt, and S. D. Kevan, Phys. Rev. Lett. **69**, 2598 (1992).

[5] P. Skytt, J.-H. Guo, N. Wassdahl, J. Nordgren, Y. Luo, and H. Ågren, Phys. Rev. A **52**, 3572 (1995).

[6] P. Glans, K. Gunnelin, P. Skytt, J.-H. Guo, N. Wassdahl, J. Nordgren, H. Ågren, F. Kh. Gel'mukhanov, T. Warwick, and E. Rotenberg, Phys. Rev. Lett. **76**, 2448 (1996).

[7] P. Morin and I. Nenner, Phys. Rev. Lett. **56**, 1913 (1986).

[8] H. Aksela, S. Aksela, M. Ala-Korpela, O. P. Sarinen, M. Hotokka, G. M. Bancroft, K. H. Tan, and J. Tulkki, Phys. Rev. A **41**, 6000 (1990).

[9] S. Aksela, H. Aksela, A. Naves de Brito, G. M. Bancroft, and K. H. Tan, Phys. Rev. A **45**, 7948 (1992).

[10] A. Naves de Brito and H. Ågren, Phys. Rev. A **45**, 7953 (1992).

[11] A. Kivimäki, H. Aksela, S. Aksela, A. Yagishita, and E. Shigemasa, J. Phys. B **26**, 3379 (1993).

[12] M. Larsson, P. Baltzer, S. Svensson, B. Wannberg, N. Mårtensson, A. Naves de Brito, N. Correia, M. P. Keane, M. Carlsson-Göthe, and L. Karlsson, J. Phys. B **23**, 1175 (1990).

[13] P. Kuiper and B. I. Dunlap, J. Chem. Phys. **100**, 4087 (1994).

[14] B. Wannberg, S. Svensson, M. P. Keane, L. Karlsson, and P. Baltzer, Chem. Phys. **133**, 281 (1989).

[15] G. S. Brown, M. H. Chen, B. Crasemann, and G. E. Ice, Phys. Rev. Lett. **45**, 1937 (1980).

[16] T. Åberg and B. Crasemann, in *X-Ray Resonant Scattering* (Ref. [3]).

[17] A. Kivimäki, A. Naves de Brito, S. Aksela, H. Aksela, O.-P. Sarinen, A. Ausmees, S. J. Osborne, L. B. Dantas, and S. Svensson, Phys. Rev. Lett. **71**, 4307 (1993).

[18] Z. F. Liu, G. M. Bancroft, K. H. Tan, and M. Schachter, Phys. Rev. A **48**, R4019 (1994).

[19] Z. F. Liu, G. M. Bancroft, K. H. Tan, and M. Schachter, Phys. Rev. Lett. **72**, 621 (1994).

[20] S. Aksela, E. Kukk, H. Aksela, and S. Svensson, Phys. Rev. Lett. **74**, 2917 (1995).

[21] F. Kh. Gel'mukhanov and H. Ågren, Phys. Rev. A **49**, 4378 (1994).

[22] F. Kh. Gel'mukhanov and H. Ågren, Phys. Rev. A **50**, 1129 (1994).

[23] Y. Luo, H. Ågren, and F. K. Gelmukhanov, J. Phys. B **27**, 4169 (1994).

[24] F. Kh. Gel'mukhanov, L. N. Mazalov, and N. A. Shklyaeva, Zh. Eksp. Teor. Fiz. **71**, 960 (1976) [Sov. Phys. JETP **44**, 504 (1975)].

[25] Y. Ma, Phys. Rev. B **49**, 5799 (1994).

[26] N. Correia, A. F. Flores, H. Ågren, K. Helenelund, L. Asplund, and U. Gelius, J. Chem. Phys. **83**, 2035 (1985).

[27] T. X. Carroll, S. E. Anderson, L. Ungier, and T. D. Thomas, Phys. Rev. Lett. **58**, 867 (1987).

[28] E. D. Poliakov, L. A. Kelly, L. M. Duffy, P. Roy, S. H. Southworth, and M. G. White, J. Chem. Phys. **89**, 4048 (1988).

[29] F. K. Gel'mukhanov, L. N. Mazalov, and A. V. Kondratenko, Chem. Phys. Lett. **46**, 133 (1977).

[30] F. Kaspar, W. Domcke, and L. S. Cederbaum, Chem. Phys. **44**, 33 (1979).

[31] A. Cesar, H. Ågren, and V. Carravetta, Phys. Rev. A **40**, 187 (1989).

[32] L. S. Cederbaum and F. Tarantelli, J. Chem. Phys. **98**, 9691 (1993).

[33] F. Kh. Gelmukhanov and H. Ågren, Phys. Lett. A **193**, 375 (1994).

[34] G. B. Armen and H. Wang, Phys. Rev. A **51**, 1241 (1995).

[35] *Handbook of Mathematical Functions*, edited by M. Abramowitz and I. Stegun (Dover, New York, 1965).

[36] D. E. Apsnes, Phys. Rev. **147**, 554 (1966).

[37] O. Goscinski, J. Müller, E. Poulain, and H. Siegbahn, Chem. Phys. **55**, 407 (1978).

[38] L. J. Saethre, S. Svensson, N. Mårtensson, U. Gelius, P. Å. Malmquist, E. Basilier, and K. Siegbahn, Chem. Phys. **20**, 431 (1977).

[39] G. Herzberg, in *Molecular Spectra and Molecular Structure. I. Spectra of Diatomic Molecules* (Van Nostrand Reinhold, London, 1950).

[40] L. D. Landau and E. M. Lifshitz, *Quantum Mechanics* (Pergamon, Oxford, 1965).

[41] H. Aksela, S. Aksela, M. Hotokka, A. Yagishita, and E. Shigemasa, J. Phys. B **25**, 3357 (1992).

[42] R. G. Newton, *Scattering Theory of Waves and Particles* (Springer-Verlag, Berlin, 1982).

[43] S. O. Lee and E. H. Heller, J. Chem. Phys. **71**, 4777 (1979).

[44] E. J. Heller, R. L. Sunberg, and D. Tannor, J. Phys. Chem. **86**, 1822 (1982).

[45] *Problems in Quantum Mechanics*, edited by D. ter Haar (Pion, London, 1975).

[46] E. Kukk, H. Aksela, S. Aksela, F. Gelmukhanov, and H. Ågren, Phys. Rev. Lett. **76**, 3100 (1996).